



Transmissible Gastroenteritis Virus Infection Promotes the Self-Renewal of Porcine Intestinal Stem Cells via Wnt/ β -Catenin Pathway

Ning Yang,^{a,b} Yunhang Zhang,^{a,b} Yuguang Fu,^a Yang Li,^{a,b} Shanshan Yang,^{a,d} Jianing Chen,^a Guangliang Liu^{a,c}

^aState Key Laboratory of Veterinary Etiological Biology, College of Veterinary Medicine, Lanzhou University, Lanzhou Veterinary Research Institute, Chinese Academy of Agricultural Sciences, Lanzhou, China

^bMolecular and Cellular Epigenetics (GIGA) and Molecular Biology (TERRA), University of Liege, Gembloux, Belgium

^cHainan Key Laboratory of Tropical Animal Breeding and Infectious Disease Research, Institute of Animal Husbandry and Veterinary Medicine, Hainan Academy of Agricultural Sciences, Haikou, China

^dCell Biology and Immunology Group, Wageningen University and Research, Wageningen, The Netherlands

ABSTRACT Intestinal stem cells (ISCs) play an important role in tissue repair after injury. A recent report delineates the effect of transmissible gastroenteritis virus (TGEV) infection on the small intestine of recovered pigs. However, the mechanism behind the epithelium regeneration upon TGEV infection remains unclear. To address this, we established a TGEV infection model based on the porcine intestinal organoid monolayer. The results illustrated that the porcine intestinal organoid monolayer was susceptible to TGEV. In addition, the TGEV infection initiated the interferon and inflammatory responses following the loss of absorptive enterocytes and goblet cells. However, TGEV infection did not disturb epithelial integrity but induced the proliferation of ISCs. Furthermore, TGEV infection activated the Wnt/ β -catenin pathway by upregulating the accumulation and nuclear translocation of β -catenin, as well as promoting the expression of Wnt target genes, such as C-myc, Cyclin D1, Mmp7, Lgr5, and Sox9, which were associated with the self-renewal of ISCs. Collectively, these data demonstrated that the TGEV infection activated the Wnt/ β -catenin pathway to promote the self-renewal of ISCs and resulted in intestinal epithelium regeneration.

IMPORTANCE The intestinal epithelium is a physical barrier to enteric viruses and commensal bacteria. It plays an essential role in maintaining the balance between the host and intestinal microenvironment. In addition, intestinal stem cells (ISCs) are responsible for tissue repair after injury. Therefore, prompt self-renewal of intestinal epithelium will facilitate the rebuilding of the physical barrier and maintain gut health. In the manuscript, we found that the transmissible gastroenteritis virus (TGEV) infection did not disturb epithelial integrity but induced the proliferation of ISCs and facilitated epithelium regeneration. Detailed mechanism investigations revealed that the TGEV infection activated the Wnt/ β -catenin pathway to promote the self-renewal of ISCs and resulted in intestinal epithelium regeneration. These findings will contribute to understanding the mechanism of intestinal epithelial regeneration and reparation upon viral infection.

KEYWORDS TGEV, Wnt/ β -catenin pathway, epithelium regeneration, intestinal organoid monolayer, intestinal stem cells

Transmissible gastroenteritis virus (TGEV), a member of the genus *Alphacoronavirus* in the family of *Coronaviridae*, is a single-stranded, positive-sense RNA virus (1). TGEV causes acute intestinal diarrhea in infected pigs, and the epidemic of TGEV leads to a huge economic loss in the global pig industry (2). The gastroenteritis caused by TGEV is characterized by watery diarrhea, vomiting, and dehydration with high morbidity and

Editor Tom Gallagher, Loyola University Chicago

Copyright © 2022 American Society for Microbiology. All Rights Reserved.

Address correspondence to Guangliang Liu, LiuGuangliang01@caas.cn.

The authors declare no conflict of interest.

Received 23 June 2022

Accepted 21 August 2022

Published 8 September 2022

mortality especially in piglets less than 2 weeks old (3). TGEV infection induces intestinal epithelial dysfunction and imbalance of intestinal homeostasis, typically with weakened cellular electrolyte absorption, and the loss of epithelium and crypt hyperplasia (3–5). Pigs of all ages are susceptible to TGEV, but adult pigs recovered from TGEV infection showed stunted growth (6). Xia et al. (3) reported that the epithelium recovered from TGEV infection maintained intestinal homeostasis. However, the molecular mechanisms responsible for this phenotype remain unknown.

As a physical barrier, the intestinal epithelium plays an essential role in maintaining the balance between the host and intestinal microenvironment, and it is susceptible to enteric viruses and commensal bacteria (7). The highly dynamic epithelial cells regenerate every 4 to 5 days in a steady-state and damage-induced intestinal regeneration is inseparable from the self-renewal and differentiation of intestinal stem cells (ISCs) (8–10). ISCs, located at the bottom of the intestinal crypt, are critical to maintaining homeostasis of the intestinal epithelium by constantly self-renewing and fueling the rapid turnover of the intestinal epithelium. The self-renewal of ISCs gives rise to transit-amplifying (TA) cells. Part of TA cells migrate upward and finally differentiate into absorptive enterocytes, goblet cells, and enteroendocrine cells to fulfill epithelial renewal, other TA cells migrate downward to remain at the bottom of the crypt and differentiate into Paneth cells (11). Injury and inflammatory responses disrupt this homeostasis of stem cell renewal and differentiation, thereby inducing a series of homeostatic imbalances accompanied by the loss of epithelial cells or hyperproliferation of crypt stem cells (12). However, to maintain homeostasis and recover from the damage, the self-renewal and differentiation of ISCs are activated for initiating epithelium regeneration (13, 14).

The canonical Wnt/ β -catenin pathway is involved in the self-renewal and differentiation of ISCs (15–17). The Wnt signaling is one of the determinants for the fate of ISCs in repair processes following injury (18), while the β -catenin is the central signal in this pathway. Upon Wnt signal ligands binding with the complex of Frizzled and lipoprotein receptor-related protein (LRP) transmembrane receptor, the degradation complex consists of the tumor suppressor axin and adenomatous polyposis coli (APC) as well as constitutively active kinases glycogen synthase kinase 3 β (GSK3 β) and casein kinase I (CK1) is inhibited then the β -catenin will be released. Subsequently, free β -catenin enters the nucleus and interacts with transcription factors of the T cell factor/lymphocyte enhancer factor (TCF/LEF). As a result, the transcriptional complex further induces the transcription of target genes, like C-myc, Cyclin D1, and matrix metalloproteinase (16, 19). Studies have shown *Salmonella* can activate Wnt/ β -catenin signaling and increase the number of ISCs. The porcine reproductive and respiratory syndrome virus (PRRSV) infection also induces the activation of the Wnt/ β -catenin pathway and high expression of β -catenin can inhibit PRRSV replication (20, 21). In addition, Zn-Asp enhances ISCs activity by activating the Wnt/ β -catenin signaling pathway and, thus, maintains the epithelial structure and barrier after deoxynivalenol treatment (22). These data suggest the association of virus infection with Wnt/ β -catenin signaling and the importance of Wnt/ β -catenin signaling in boosting epithelial renewal.

In our previous study, we demonstrated that porcine ileal apical-out organoids were susceptible to TGEV and induced a series of antiviral and inflammatory responses (23). To better explore the impact of TGEV on the epithelium, we developed a porcine intestinal organoid monolayer culture system that contains multiple epithelial cell subsets in this study. With these monolayer cultures, we investigated the susceptibility of an organoid monolayer to TGEV infection. The antiviral responses and the integrity of intestinal epithelium after TGEV infection were also evaluated. Simultaneously, we explored the effects of TGEV infection on ISC development and correlative molecular mechanisms. The results demonstrated that the organoid monolayer was susceptible to TGEV infection, which induced the interferon and inflammatory responses without changing the epithelial integrity. Moreover, TGEV infection increased the self-renewal of ISCs by activating Wnt/ β -catenin signaling to initiate epithelium regeneration.

RESULTS

Development of 3D porcine intestinal organoids. Porcine intestinal crypts were isolated from the intestinal follicle-associated epithelium of the ileum following the previous protocol (23), then cultured in Matrigel supplemented with organoid growth medium (OGM) (Fig. S1A in Supplemental File 1). The formation of crypt-villus structures was observed after culturing for 12 days (Fig. S1B in Supplemental File 1), which harbored different epithelial cell subsets and ISCs. When passaging the organoids, the budding organoid was observed after 3 days of culturing (Fig. S1C in Supplemental File 1). In addition, the immunofluorescence assay (IFA) result showed that a large amount of Ki67⁺ and Sox9⁺ cells were observed in the organoids cultured for 5 days, indicating their proliferative capacity and stemness (Fig. S1D in Supplemental File 1).

Establishment of the porcine intestinal organoid monolayer. Intestinal organoid monolayer has been widely used to study the interaction between host and enteric virus (24). To investigate the TGEV infection, we developed the porcine intestinal organoid monolayer culture system through dissociating 3D intestinal organoids into single cells or small fragments and culturing in Transwell plate (Fig. 1A). Subsequently, the confluent intestinal organoid monolayer was observed after 3 days culturing (Fig. 1B). Meanwhile, the porcine intestinal epithelial barrier was successfully established, showing a transepithelial electrical resistance (TER) value between 145 and 160 Ω/cm^2 (Fig. 1C). In addition, different intestinal epithelial cell subsets, absorptive enterocyte (Villin positive), proliferating cells (Ki67 positive), Paneth cell (LYZ positive), enteroendocrine cells (CGA positive), goblet cells (Muc2 positive) and stem cells (Sox9 positive) and tight junction protein of epithelial cells (ZO-1) were successfully detected in this monolayer culture system (Fig. 1D). These above results indicated that the intestinal organoid monolayer system possessed epithelial integrity and complex multicellularity after 3 days culturing.

Porcine intestinal organoid monolayer was susceptible to TGEV. To investigate whether the porcine intestinal organoid monolayer is valid to explore the interactions between the intestinal epithelial cells and enteric viruses, the TGEV was employed to infect the porcine intestinal organoid monolayer. The results of the reverse transcription-quantitative PCR (RT-qPCR) and the 50% tissue culture infective dose (TCID₅₀) assay demonstrated that the organoid monolayer system was susceptible to TGEV. The viral load peaked at 36 h postinfection (hpi) and subsequently decreased at 48 hpi, and the viral titer measured on ST cells also peaked at 36 hpi (Fig. 2A and B). In addition, the IFA results indicated that the expression of TGEV N on intestinal organoid monolayer can be observed at 24 hpi (Fig. 2C). Consistent with this finding, the Western blot also exhibited the presence of TGEV N protein (Fig. 2D) and upregulation of Aminopeptidase N (APN) expression (Fig. 2E), the primary receptor for TGEV infection. To further explore the antiviral responses of an organoid monolayer, the transcriptional expression levels of interferons, interferon-stimulated genes, as well as inflammatory factors induced by TGEV infection were evaluated by RT-qPCR. The results illustrated that the TGEV infection significantly stimulated the transcription of interferon (IFN)- λ 1, IFN- λ 3, and IFN- γ . Meanwhile, the mRNA level of interferon-stimulated gene 15 (ISG15) and interferon-stimulated gene 58 (ISG58) were also elevated (Fig. 2F). Furthermore, the transcription levels of interleukin (IL)-8, IL-6, and tumor necrosis factor (TNF)- α were significantly upregulated (Fig. 2F). These data suggested that the IFNs and inflammatory responses were initiated by TGEV infection. Next, we determined the target cells of TGEV infection on the intestinal organoid monolayer. The colocalization results revealed that TGEV infected part of Villin⁺ cells (absorptive enterocytes) and Ki67⁺ cells (proliferation cells) (Fig. 2G). Besides, the IFA result showed that TGEV infection downregulated the number of Villin⁺ cells (absorptive enterocytes), but there was no significant difference in Ki67⁺ cells (proliferation cells) (Fig. S2 in Supplemental File 1). This part of the results suggested that the porcine intestinal organoid monolayer culture system is susceptible to TGEV, a swine enteric virus.

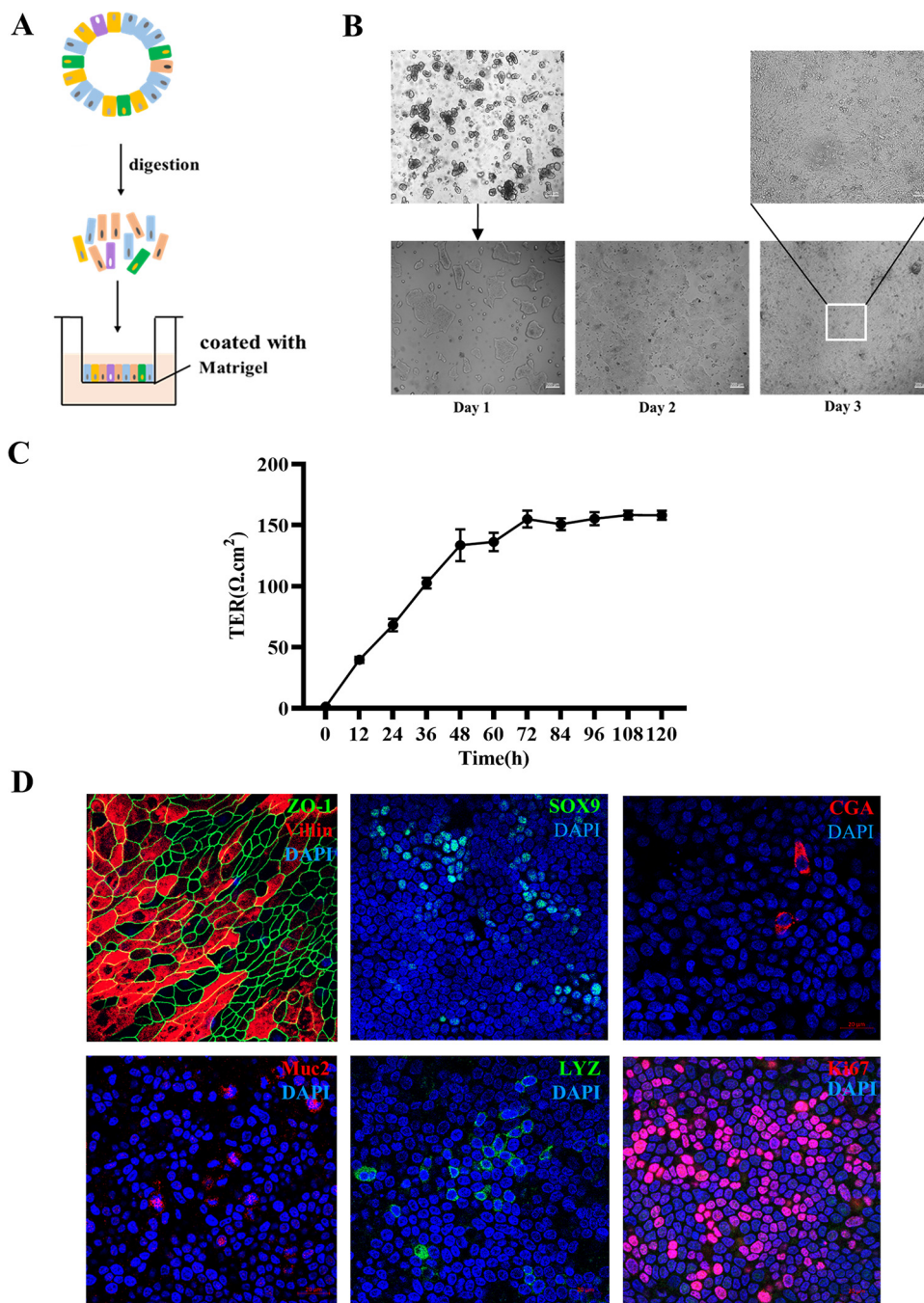


FIG 1 Establishment of a porcine intestinal organoid monolayer. (A) Graphical representation for the establishment of an organoid monolayer. (B) Single cells grow into a confluent monolayer after seeding for 3 days. (C) Transepithelial electrical resistance (TER) was measured during the development of an organoid monolayer. Values were from three independent monolayers. (D) Organoid monolayer was subjected to IFA staining for absorptive enterocytes (Villin), tight junction (ZO-1), stem cells (Sox9), enteroendocrine cells (CGA), goblet cells (Muc2), Paneth cells (LYZ), and proliferation cells (Ki67).

TGEV infection maintained the epithelial integrity of an intestinal organoid monolayer. To identify whether the TGEV infection affects the epithelial integrity of the organoid monolayer system, the TER was evaluated. The results showed that TGEV infection did not change the TER value of the intestinal organoid monolayer culture system, indicating it didn't disrupt the epithelial integrity of this system (Fig. 3A). In addition, the ZO-1, a critical protein involved in the tight junction of epithelial cells, was stained to additionally identify if TGEV infection affects the integrity of the intestinal organoid monolayer. Again, the result demonstrated that TGEV didn't change the expression

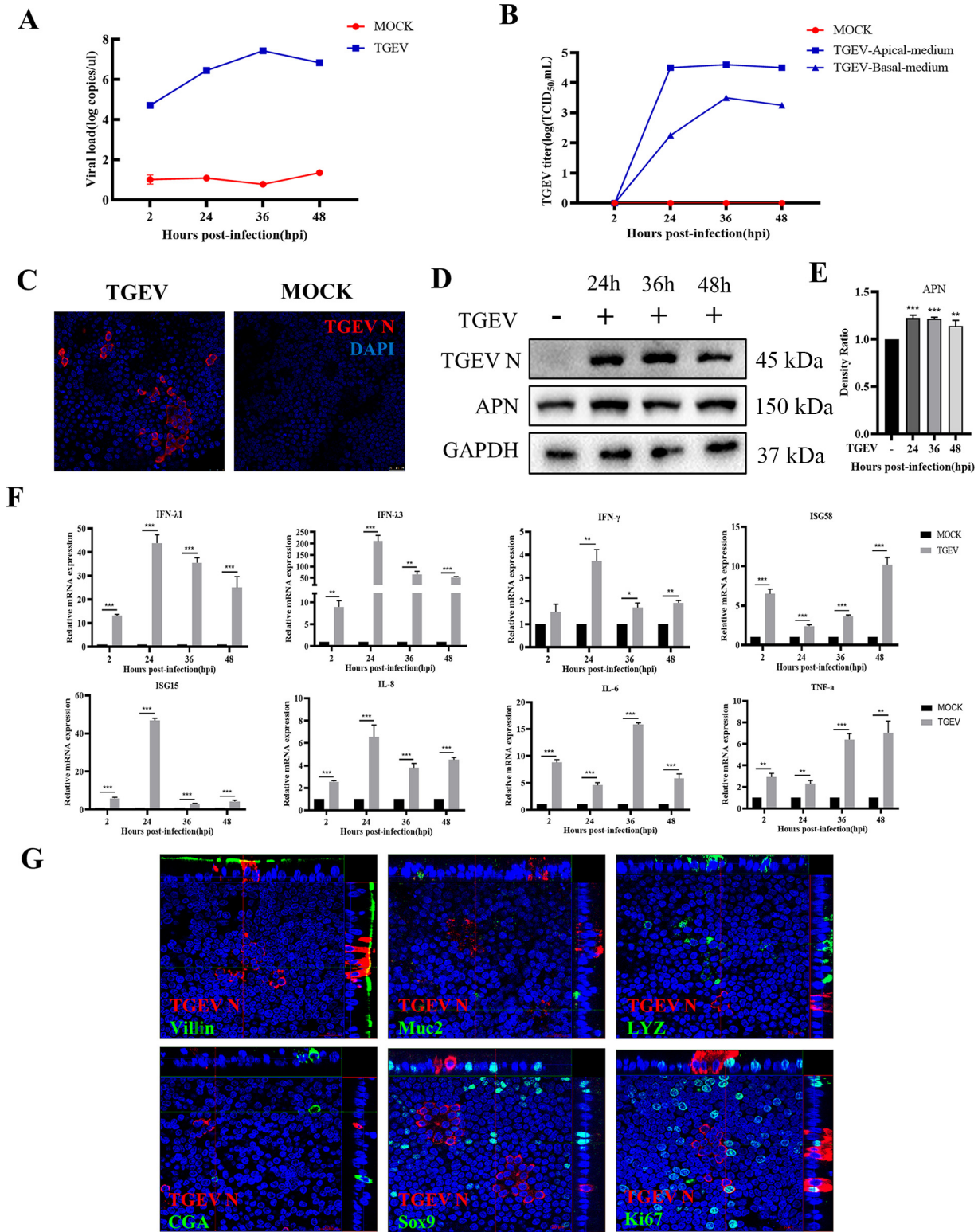


FIG 2 Porcine intestinal organoid monolayer is susceptible to TGEV. (A) The kinetics of TGEV replication porcine intestinal organoid monolayer at the indicated time points were measured by RT-qPCR. (B) The TGEV titers in supernatant from both the apical side and basal side of the Transwell-cultured organoid monolayer were titrated by TCID₅₀ assay on the ST cell lines. (C) Organoid monolayer infected with TGEV for 24 h was stained with TGEV N monoclonal antibody. (D) The expression of TGEV N and APN were detected by Western blotting. (E) The density ratio of APN expression was calculated with Image J and normalized against GAPDH expression. **, $P \leq 0.01$; ***, $P \leq 0.001$. (F) The transcription levels of IFN-λ1, IFN-λ3, IFN-γ, ISG58, ISG15, IL-8, IL-6, and TNF-α in organoid monolayer after TGEV infection were evaluated by RT-qPCR. The RT-qPCR data were calculated using the comparative threshold cycle ($2^{-\Delta\Delta CT}$) method. *, $P \leq 0.05$; **, $P \leq 0.01$; ***, $P \leq 0.001$. (G) Colocalization analysis of TGEV N with different epithelial cell subsets and proliferation cells was performed by confocal microscopy.

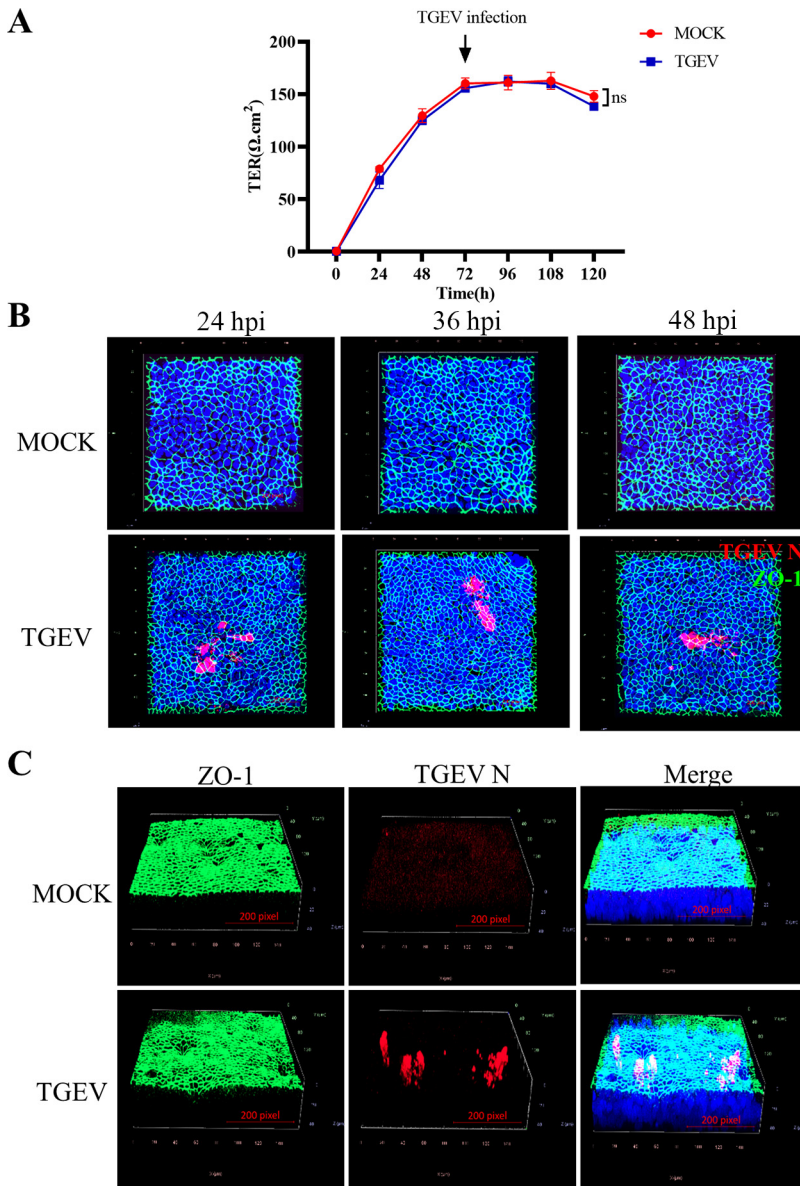


FIG 3 TGEV infection maintains epithelial integrity in intestinal organoid monolayer. (A) Transepithelial electrical resistance (TER) value in organoid monolayer infection was measured after TGEV infection. Values were from three independent monolayers. (B) TGEV-infected or mock-infected intestinal organoid monolayer at 24 hpi, 36 hpi, and 48 hpi were stained with ZO-1 and TGEV N and observed by confocal microscopy. (C) TGEV-infected or mock-infected intestinal organoid monolayers at 7 dpi were stained with ZO-1 and TGEV N and analyzed by 3D imaging of confocal microscopy.

pattern of ZO-1 at indicated infection time points and 7 dpi (Fig. 3B and C), further approving the organoid monolayer maintained its integrity after TGEV infection.

TGEV infection promoted the self-renewal of intestinal stem cells. ISCs play an essential role in epithelium renewal after injury or inflammation. We speculated that the TGEV infection induced the activation of ISCs to maintain the integrity of the organoid monolayer. To verify our hypothesis, the expression level of Sox9, an essential marker of ISCs, was evaluated by Western blotting and IFA analysis. The Western blot showed that TGEV infection significantly upregulated the expression of Sox9 at 24 hpi and thereafter (Fig. 4A and B). In addition, the IFA analysis further delineated that TGEV infection elevated the number of Sox9⁺ cells (Fig. 4C), and the value of mean fluorescence intensity in TGEV infection at 24 hpi was significantly higher than the mock group (Fig. 4D), indicating that TGEV infection indeed induced the self-renewal of ISCs

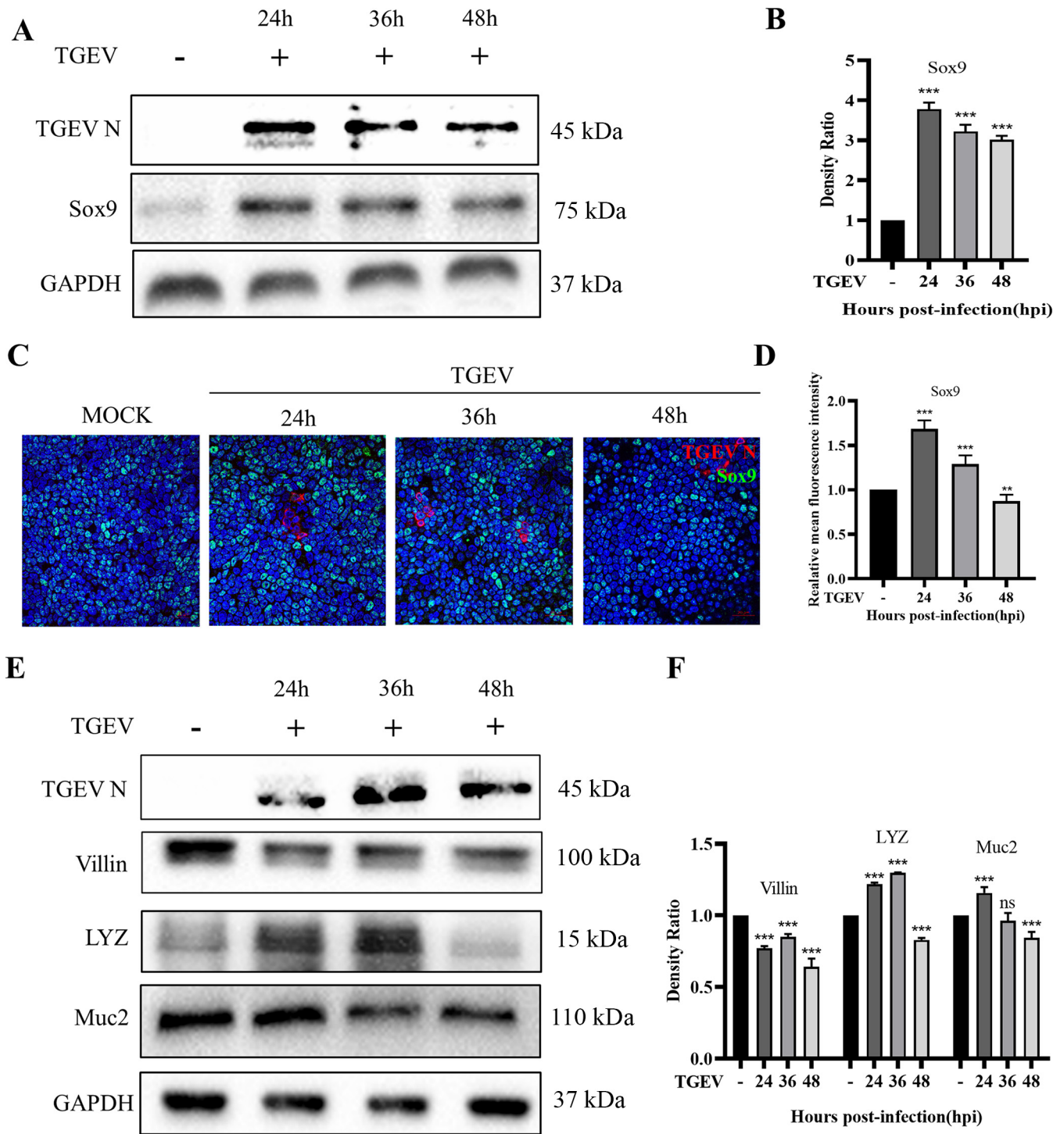


FIG 4 TGEV infection promoted the self-renewal of ISCs. (A) The expression of Sox9, representing the number of ISCs, was detected by Western blotting. (B) The density ratio of Sox9 expression was calculated with Image J and normalized against GAPDH expression. (C) Sox9 and TGEV N were stained in intestinal organoid monolayer at indicated time points and observed under confocal microscopy. (D) The mean fluorescence intensity of Sox9⁺ cells in organoid monolayer infected with TGEV was analyzed. The data from five independent stainings. (E) The expression of Villin, LYZ, and Muc2 was detected by Western blotting, which represents absorptive enterocytes, Paneth cells, and goblet cells, respectively. (F) The density ratios of Villin, LYZ, and Muc2 were calculated with Image J and normalized against GAPDH expression. ns, not significant; **, $P \leq 0.01$; ***, $P \leq 0.001$.

in the organoid monolayer culture system. Moreover, the expression levels of other main intestinal epithelial cell subsets were also measured by Western blotting. The result showed that absorptive enterocytes (Villin⁺) and goblet cells (Muc2⁺) were decreased after TGEV infection, but Paneth cells were increased after TGEV infection

for 36h (Fig. 4D and E). However, the enteroendocrine cells were not detected in this study, which may be related to their low percentage in the intestinal epithelium. Collectively, those data suggested that the TGEV infection led to the loss of absorptive enterocytes and goblet cells but induced the self-renewal of ISCs. Besides, the increase of Paneth cells implied a special relationship with ISCs (25).

TGEV infection activated the Wnt/ β -catenin pathway in an intestinal organoid monolayer. The Wnt/ β -catenin pathway, a crucial signal for the proliferation and differentiation of ISCs, was reported also involves in epithelium repair after injury (26). We hypothesized that the TGEV infection promoted ISC self-renewal via the Wnt/ β -catenin pathway. To testify this speculation, the relative expression levels of critical components in this pathway were measured by RT-qPCR. The results revealed that the TGEV infection significantly upregulated the mRNA transcription levels of Wnt3a, β -catenin, TCF4, Cyclin D1, C-myc, Mmp7, Lgr5, and Sox9 (Fig. 5A). Simultaneously, the Western blot also indicated that TGEV infection promoted the accumulation of β -catenin and the upregulations of Cyclin D1 and C-myc expressions (Fig. 5B and C). Furthermore, the IFA results confirmed the ectopic expression of β -catenin. The nuclear translocation of β -catenin was observed after TGEV infection at 24 hpi in an organoid monolayer (Fig. 5D). These results indicated that the TEGV infection activated the Wnt/ β -catenin pathway to promote the self-renewal of ISCs.

TGEV infection promoted the self-renewal of porcine intestinal stem cells via the Wnt/ β -catenin pathway. The activation of the Wnt/ β -catenin pathway depends on the accumulation of β -catenin and interaction with TCF/LEF and, finally, that initiates the transcription of Wnt target genes (15). To further identify that the TGEV infection promoted ISC self-renewal via the Wnt/ β -catenin pathway, the ICG-001 (HY-14428; MCE, USA), a small molecule inhibitor for the Wnt/ β -catenin pathway, was employed in our organoid monolayer system. This molecule can block the interaction between β -catenin and creb-binding protein (CBP) thereby repressing β -catenin/TCF-mediated transcription. First, the ICG-001 treatment dosing and timing were optimized. The result displayed that the Wnt/ β -catenin pathway was effectively inhibited by treatment with 10 μ M ICG-001 for 24 h (Fig. 6A and B). Next, the organoid monolayer was treated with 10 μ M ICG-001 for 24 h before TGEV infection, and the expression of C-myc and the development of ISCs were evaluated. The result illustrated that TGEV infection reversed the inhibition of the Wnt/ β -catenin pathway and ISCs self-renewal caused by ICG-001 (Fig. 6C and D). Collectively, these data revealed that the TGEV infection promoted the self-renewal of ISCs via the Wnt/ β -catenin signaling pathway.

DISCUSSION

Intestinal organoids derived from Lgr5⁺ stem cells were first proposed in 2009 (27). Due to the organoid system better mimicking the multiple cell types than conventional cell lines, it was widely used to study the interactions between host and pathogen (28). In our previous study, we developed a porcine apical-out intestinal organoid culture system, and it was susceptible to TGEV and induced an antiviral response (23). Xia et al. (3) reported that TGEV infection damaged the small intestine, inhibited mucosal immune responses, and elevated inflammatory response, but enhanced ISCs proliferation in the recovered pig. In this study, we developed a porcine intestinal organoid monolayer culture system to investigate the antiviral response of TGEV, the impact of TGEV on epithelial integrity, epithelial cell subsets fate, and the mechanism of epithelium regeneration. Our results demonstrated that TGEV was able to infect the intestinal organoid monolayer and induced the interferon (IFN) antiviral responses, especially IFN- λ . Meantime, the expression of inflammatory factors, such as IL-8, IL-6, and TNF- α , was significantly upregulated. These results were consistent with previous reports (23, 29). In addition, we found that TGEV can infect partially absorptive enterocytes and proliferation cells, leading to the loss of absorptive enterocytes and goblet cells. These data clarify the reason for impaired intestinal absorption and loss of villous epithelium after TGEV infection (3). Goblet cells, a group of secretory epithelial cells that produce mucus, can effectively prevent pathogen invasion (30). We speculate the loss of goblet

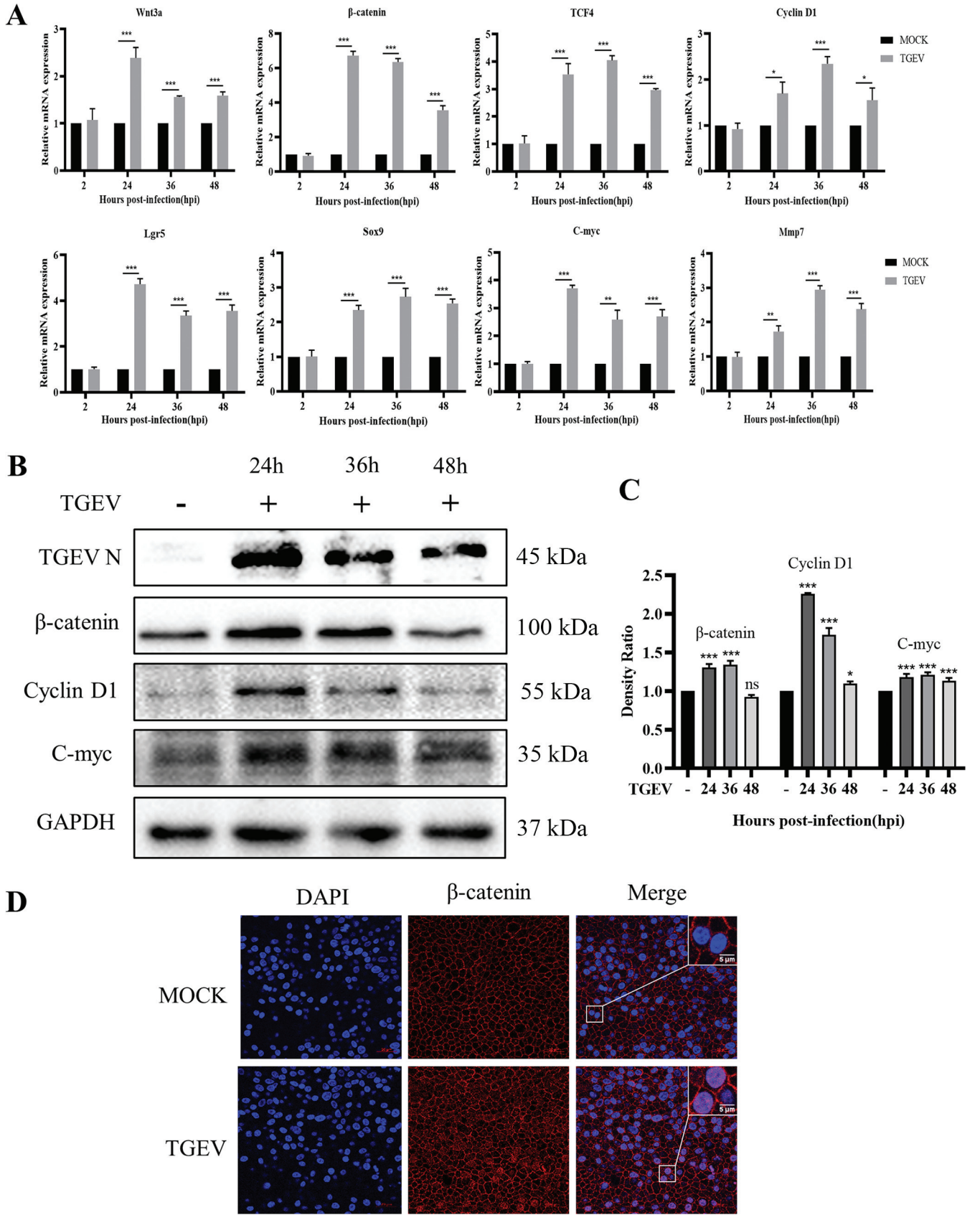
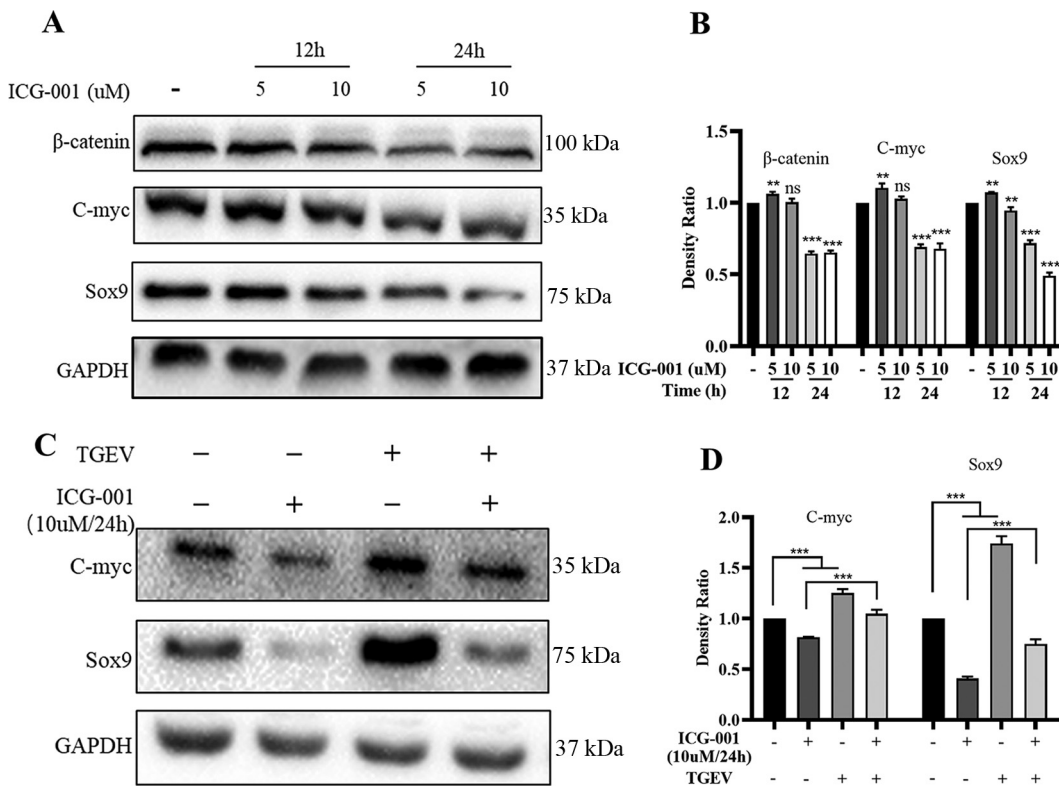


FIG 5 TGEV infection activated the Wnt/ β -catenin pathway. (A) The transcription levels of Wnt3a, β -catenin, TCF4, Cyclin D1, Lgr5, Sox9, C-myc, and Mmp7 in organoid monolayer were measured by RT-qPCR after TGEV infection. The RT-qPCR data were calculated using the comparative threshold cycle ($2^{-\Delta\Delta CT}$)

(Continued on next page)



cells induced by TGEV is potentially responsible for the increased susceptibility to pathogens in the intestinal epithelium.

It is well known that ISCs are the dominant force in the rapid renewal of intestinal epithelium. They possess self-renewal and multilineage differentiation potential to maintain epithelium homeostasis and repair injured epithelium (31). In previous studies, investigators demonstrated that the proliferation of ISCs is a repair mechanism in response to the damaged intestinal epithelium, and an unknown signal involved in damaged epithelial cells induced stem cell proliferation (13, 32). *Salmonella* and *Erwinia carotovora* induced the activation and division of ISCs via different signaling (13, 20). Similarly, our result elucidated that the TGEV infection promoted the self-renewal of ISCs and resulted in the repair of epithelium after infection. In addition, TGEV infection also increased the differentiation of Paneth cells transiently. Paneth cells are in the bottom of the crypt, intercalated between ISCs, and serve as a stem cell niche (25). A previous report showed the Paneth cells govern ISCs renewal and regeneration following homeostasis or injury (33).

The Wnt pathway is essential for the proliferation and maintenance of ISCs (34, 35). The epithelial Wnt derived from Paneth cells forms the epithelial Wnt gradient for the maintenance of stem cells (33). In our study, TGEV infection significantly upregulated the expression of β -catenin and Wnt target genes, such as C-myc, cyclin D1, and Mmp7. Wnt3a is an

FIG 5 Legend (Continued)

method. *, $P \leq 0.05$; **, $P \leq 0.01$; ***, $P \leq 0.001$. (B) The expression of β -catenin, Cyclin D1, and C-myc in organoid monolayer was detected by Western blotting after TGEV infection. (C) The density ratios of β -catenin, Cyclin D1, and C-myc were calculated with Image J and normalized against GAPDH expression. ns, not significant; *, $P \leq 0.05$; ***, $P \leq 0.001$ (D) The nuclear translocation of β -catenin was observed in organoid monolayer by confocal microscopy after TGEV infection (bar = 20/5 μ m).

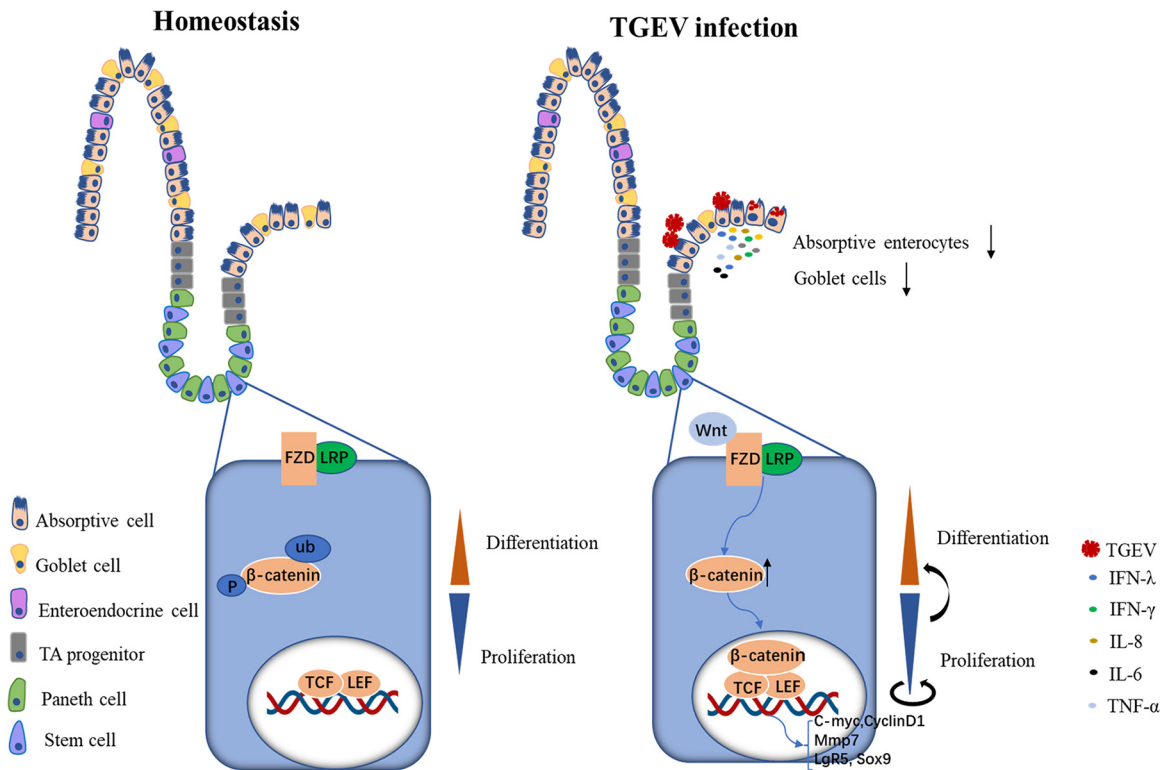


FIG 7 Schematic diagram of TGEV-induced intestinal epithelial regeneration via Wnt/ β -catenin pathway.

activator of the canonical Wnt/ β -catenin pathway and it is mainly derived from Paneth cells *in vivo* (33). TGEV infection significantly increased the transcription of Wnt3a, which activated the Wnt/ β -catenin signaling. Similarly, an investigation showed that *Salmonella* infection increased the number of stem cells and proliferative cells through the activation of the Wnt/ β -catenin signaling pathway (20). In addition, recent reports also discussed the effort of inflammatory factors on the self-renewal and differentiation of stem cells (32, 36, 37). Damaged *Drosophila* intestinal epithelium express IL-6, which in turn activates the Jak/Stat pathway in the ISCs and promotes the differentiation to achieve repair of the damaged epithelium (32). IL-22 has also been linked to ISC-mediated epithelial regeneration and regeneration of the ISC pool (36). Besides, the Wnt/ β -catenin signaling pathways were activated to promote the malignant transformation of ISCs in TNF- α -induced inflammatory responses (37). Considering this, we speculate that the TGEV-induced proinflammatory factors may facilitate the self-renewal of stem cells and ISCs-mediated epithelial regeneration.

To conclude, we revealed that the TGEV was infective to porcine intestinal organoid monolayer and triggered the self-renewal of ISCs, which further initiated the epithelial regeneration (Fig. 7). Briefly, in homeostasis, the rapid turnover of intestinal epithelium depended on the support of intestinal crypt stem cells. An exquisite balance was established between the proliferation of stem cells and the generation of differentiated offspring. However, upon TGEV infection, parts of absorptive enterocytes were infected and responded to viral infection, which caused the loss of different epithelial cells. Meantime, TGEV infection activated the Wnt/ β -catenin pathway and, therefore, promoted the self-renewal of ISCs, which further accelerated the differentiation of offspring and completes epithelium regeneration. These findings contribute to understanding the mechanism of intestinal epithelial regeneration and reparation upon viral infection.

MATERIALS AND METHODS

Virus and animals. The TGEV H165 strain was previously recovered from a commercialized attenuated live vaccine (23) and stored at -86°C until use. Porcine intestines for crypts isolation were obtained from Luoniushan slaughterhouse, Hainan province.

TABLE 1 List of antibodies used in this study

Antibody	Type	Supplier	Product no.
Ki-67	Mouse	BD Biosciences	550609
Sox9	Rabbit	CST	82630
Villin	Mouse	Santa Cruz	SC-58897
ZO-1	Rabbit	Invitrogen	PA5-85256
CGA	Mouse	Santa Cruz	sc-393941
Muc2	Rabbit	Abcam	ab134119
LYZ	Rabbit	Invitrogen	PA5-16668
β -catenin	Rabbit	CST	8480
APN	Rabbit	Abconal	A5662
C-myc	Rabbit	ZENBIO	343250
Cyclin D1	Rabbit	CST	2922
GAPDH	Rabbit	Proteintech	10494-1-AP

Porcine intestinal 3D organoids culture. Porcine ileum crypts were isolated and cultured in 3D organoids culture system with the support of Matrigel (Corning, USA; catalog number 356231) and the Organoids Growth Medium (OGM; StemCell, Canada; catalog number 06010) which contains 10 μ M ATP-competitive inhibitor of Rho-associated kinases (Y-27632; CST, USA; catalog number 72302) following the protocol described previously (23). Fresh medium was replaced every 2 days. The differentiated organoids (culture for 5 days) were used for the next experiment.

Porcine intestinal organoid monolayer culture. The 3D ileum organoids cultured for 5 days were collected using ice-cold DMEM/F12 (Sigma, USA; catalog number D8437) medium and centrifuged at $250 \times g$ for 5 min. The organoids pellet without Matrigel was generated by washing twice with an ice-cold DMEM/F12 medium. TrypLE Express (Gibco, USA; catalog number 12605-010), a gentle dissociation medium, was used to disassociate organoids into single cells or small fragments. The organoids were incubated with TrypLE Express for 10 min at 37°C and pipette up and down to release the organoids every 5 min. The dissociation process was aborted by DMEM/F12 with 20% FBS (Invigentech, USA; catalog number A6901FBS). Single cells or small fragments were resuspended with OGM (with 10 μ M Y-27632) and seeded into a precoated Transwell (Corning, USA; catalog number 3413) with 1.5% Matrigel at a density of 1.5×10^5 cells/well. The upper chamber of Transwell contained 200 μ L OGM with 10 μ M Y-27632, and the lower chamber contained 500 μ L OGM. Monolayer reached confluence after 3 days of culture and was used for the follow-up experiment.

Transepithelial electrical resistance. Transepithelial electrical resistance (TER) of the porcine intestinal organoid monolayer in a Transwell was measured using the epithelial volt-ohm meter (Millicell ERS-2, Merck, USA). Cells were equilibrated at room temperature for 30 min before measurement. The electrode tip was washed with 70% ethanol and DMEM/F12, respectively. Afterward, it was inset vertically into Transwell and the resistance value was recorded. An empty Transwell with OGM (200 μ L in the upper chamber; 500 μ L in the lower chamber) was used as a control group. The valid resistance value of the organoid monolayer was calculated by subtracting the resistance of the control group, and the final resistance value in $\Omega \text{ cm}^2 = \text{valid resistance value} \times \text{membrane area}$ (0.33 cm^2).

Virus infection. Organoid monolayers cultured for 3 days were washed three times with phosphate buffer saline (PBS) and then inoculated with the TGEV H165 strain (MOI = 1) or mock-infected (ST cells supernatant) for 2 h at 37°C. The residual viruses were removed by washing with PBS. Then the organoid monolayer was cultured with OGM (with 10 μ M Y-27632) for indicated times.

Immunostaining. Organoid monolayer was washed three times with PBS and fixed with 4% paraformaldehyde for 20 min at room temperature, permeabilized with 0.2% Triton X-100 (Beyotime, China; catalog number ST797) for 20 min at room temperature, and blocked with 5% BSA (Biofrox, Germany; catalog number 4240GR100) for 1 h. Primary antibodies were diluted with PBS and 5% BSA then incubated at 4°C overnight. After rinsing, secondary antibodies were diluted with PBS and incubated for 1 h at room temperature. The antibodies used in this study are listed in Table 1. Next, the nucleus of the organoid monolayer was stained with 4',6-diamidino-2-phenylindole (DAPI; Beyotime, China; catalog number C1006). The Transwell membranes were cut out using a surgical blade after washing with PBS and placed on a glass slide for imaging. The slide was observed using confocal microscopy (Zeiss LSM 900, Germany).

RNA extraction and quantitative real-time PCR. Total RNA from organoid monolayer in the Transwell was extracted using RNAiso reagent (TaKaRa, Japan; catalog number 9109), and cDNA synthesized was performed using Honor II 1st Strand cDNA Synthesis SuperMix (Vazyme, China; catalog number R223-01). The TGEV virus copy number was measured by the TaqMan probe-based RT-qPCR developed previously in our laboratory (38). The relative gene expression levels were also determined using the Unique Aptamer qPCR SYBR green master mix (Vazyme, China; catalog number Q311-02), and calculated with the $2^{-\Delta\Delta\text{CT}}$ method. The primers and probes used in this study are listed in Table 2.

Western blot. Organoid monolayer in Transwell was lysed using NP-40 (Beyotime, China; catalog number P0013F) with PMSF (Beyotime, China; catalog number ST506) for 20 min at 4°C and centrifuged at $10000 \times g$ for 5 min to remove unlysed cell debris. The protein was separated by SDS-PAGE and transferred onto a PVDF (GE, USA; catalog number 10600023) membrane. After blocking with 5% BSA, the membrane was immunoblotted overnight at 4°C with the primary antibodies (Table 1). Subsequently, the secondary antibody was incubated with the membrane for 1 h at room temperature. Finally, the

TABLE 2 Primers for real-time qPCR

Names	Primer or probe	Sequence (5'–3')
TGEV N	Forward	TGCCATGAACAAACCAAC
	Reverse	GGCACTTTACCATCGAAT
	Probe	HEX-TAGCACCACGACTACCAAGC-BHQ1 α
IFN- λ 1	Forward	CCACGTCGAACTTCAGGCTT
	Reverse	ATGTGCAAGTCTCCACTGGT
IFN- λ 3	Forward	GCCAAGGATGCCTTGAAGAG
	Reverse	CAGGACGCTGAGGGTCAGG
IFN- γ	Forward	TGGTAGCTCTGGAAACTGAATG
	Reverse	TGGCTTTGCGCTGGATCT
ISG58	Forward	CCGTGGAGCGAGACTCTATG
	Reverse	ATGTTCTCCAGACGAAGGGC
ISG15	Forward	GGTGAGGAACGACAAGGGTC
	Reverse	GGCTTGAGGTCATACTCCCC
IL-8	Forward	TCCTGCTTTCTGCAGCTCTC
	Reverse	GGGTGAAAGGTGTGGAATG
IL-6	Forward	AATGCTTTCACCTCTCC
	Reverse	TCACACTTCTCATACTTCTCA
TNF- α	Forward	GTCTCAAACCTCAGATAAG
	Reverse	GTTGTCTTTCAGCTTCAC
Wnt3a	Forward	GAGTGCCAACACCAGTTCC
	Reverse	AGTCACAGCGAAGGCAACTC
β -catenin	Forward	GACCATGCCATGATTGGACCTGAG
	Reverse	GCCTGTCAACCTTCTCGCTGTC
TCF4	Forward	TAATGGAGCAAAGGTCGTC
	Reverse	CCTGGTTTGGGACAAGAGAA
C-myc	Forward	CTCGACTCTCTGCTCTCCT
	Reverse	TTGTTCTTCTCAGAGTCGCT
Cyclin D1	Forward	GCCCTCCGTGCTACTTCA
	Reverse	AGACCTCCTCCTCGACTTCT
Mmp7	Forward	TTTCGCCTGCCTATAACTGGA
	Reverse	TTGGCTGGCTTGGGAATAG
Lgr5	Forward	CCTTGGCCCTGAACAAAATA
	Reverse	ATTTCTTTCCAGGGAGTGG
Sox9	Forward	CGGTTTCGAGCAAGAATAAGC
	Reverse	GTAATCCGGGTGGTCTTCT

protein expression was visualized with chemiluminescence detection reagents (Advansta, USA; catalog number K-12045-D50), and Image J was used to calculate the density ratio.

Statistical analysis. The data from three independent biological replicates were presented as the means \pm standard deviations (SDs). The statistical analysis was performed by two-way analysis of variance (ANOVA) or Student's *t* test with GraphPad Prism 7 software and are shown as *P* values.

SUPPLEMENTAL MATERIAL

Supplemental material is available online only.

SUPPLEMENTAL FILE 1, PDF file, 0.3 MB.

ACKNOWLEDGMENTS

We thank Li Feng from Harbin Veterinary Research Institute, Chinese Academy of Agricultural Sciences for providing a TGEV monoclonal antibody. This work was supported by the National Natural Science Foundation of China (31972689) and ULg-CAAS joint Ph.D. Program.

G.L., N.Y., and Y.F. conceived the project. N.Y., Y.Z., S.Y., and Y.L. performed the experiments. N.Y., G.L., Y.F., and J.C. analyzed the data. Y.F. drafted the manuscript. GL and NY edited the manuscript.

We declare no conflict of interest.

REFERENCES

- Zhao X, Bai X, Guan L, Li J, Song X, Ma X, Guo J, Zhang Z, Du Q, Huang Y, Tong D. 2018. microRNA-4331 promotes transmissible gastroenteritis virus (TGEV)-induced mitochondrial damage via targeting RB1, upregulating interleukin-1 receptor accessory protein (IL1RAP), and activating p38 MAPK pathway in vitro. *Mol Cell Proteomics* 17:190–204. <https://doi.org/10.1074/mcp.RA117.000432>.

2. Cui J, Li F, Shi ZL. 2019. Origin and evolution of pathogenic coronaviruses. *Nat Rev Microbiol* 17:181–192. <https://doi.org/10.1038/s41579-018-0118-9>.
3. Xia L, Yang Y, Wang J, Jing Y, Yang Q. 2018. Impact of TGEV infection on the pig small intestine. *Virology* 15:102. <https://doi.org/10.1186/s12985-018-1012-9>.
4. Yang Z, Ran L, Yuan P, Yang Y, Wang K, Xie L, Huang S, Liu J, Song Z. 2018. EGFR as a negative regulatory protein adjusts the activity and mobility of NHE3 in the cell membrane of IPEC-J2 cells with TGEV infection. *Front Microbiol* 9:2734. <https://doi.org/10.3389/fmicb.2018.02734>.
5. Xia L, Dai L, Zhu L, Hu W, Yang Q. 2017. Proteomic analysis of IPEC-J2 cells in response to coinfection by porcine transmissible gastroenteritis virus and enterotoxigenic *Escherichia coli* K88. *Proteomics Clin Appl* 11. <https://doi.org/10.1002/prca.201600137>.
6. Timoney JF, Gillespie JH, Scott FW, Barlough JE. 1988. Hagan and Bruner's Microbiology and Infectious Diseases of Domestic Animals. Cornell University Press.
7. Wang Q, Vlasova AN, Kenney SP, Saif LJ. 2019. Emerging and re-emerging coronaviruses in pigs. *Curr Opin Virol* 34:39–49. <https://doi.org/10.1016/j.coviro.2018.12.001>.
8. Zhao Q, Guan J, Wang X. 2020. Intestinal stem cells and intestinal organoids. *J Genet Genomics* 47:289–299. <https://doi.org/10.1016/j.jgg.2020.06.005>.
9. Barker N. 2014. Adult intestinal stem cells: critical drivers of epithelial homeostasis and regeneration. *Nat Rev Mol Cell Biol* 15:19–33. <https://doi.org/10.1038/nrm3721>.
10. Pitsouli C, Apidianakis Y, Perrimon N. 2009. Homeostasis in infected epithelia: stem cells take the lead. *Cell Host Microbe* 6:301–307. <https://doi.org/10.1016/j.chom.2009.10.001>.
11. Santos AJM, Lo YH, Mah AT, Kuo CJ. 2018. The intestinal stem cell niche: homeostasis and adaptations. *Trends Cell Biol* 28:1062–1078. <https://doi.org/10.1016/j.tcb.2018.08.001>.
12. Zeitz M, Ullrich R, Schneider T, Kewenig S, Hohloch K, Riecken EO. 1998. HIV/SIV enteropathy. *Ann N Y Acad Sci* 859:139–148. <https://doi.org/10.1111/j.1749-6632.1998.tb11118.x>.
13. Buchon N, Broderick NA, Poidevin M, Pradervand S, Lemaitre B. 2009. Drosophila intestinal response to bacterial infection: activation of host defense and stem cell proliferation. *Cell Host Microbe* 5:200–211. <https://doi.org/10.1016/j.chom.2009.01.003>.
14. Stewart AS, Schaaf CR, Luff JA, Freund JM, Becker TC, Tufts SR, Robertson JB, Gonzalez LM. 2021. HOPX(+) injury-resistant intestinal stem cells drive epithelial recovery after severe intestinal ischemia. *Am J Physiol Gastrointest Liver Physiol* 321:G588–G602. <https://doi.org/10.1152/ajpgi.00165.2021>.
15. Clevers H, Loh KM, Nusse R. 2014. Stem cell signaling. An integral program for tissue renewal and regeneration: Wnt signaling and stem cell control. *Science* 346:1248012. <https://doi.org/10.1126/science.1248012>.
16. Nusse R, Fuerer C, Ching W, Harnish K, Logan C, Zeng A, ten Berge D, Kalani Y. 2008. Wnt signaling and stem cell control. *Cold Spring Harbor Symp Quant Biol* 73:59–66. <https://doi.org/10.1101/sqb.2008.73.035>.
17. Guezguez A, Pare F, Benoit YD, Basora N, Beaulieu JF. 2014. Modulation of stemness in a human normal intestinal epithelial crypt cell line by activation of the WNT signaling pathway. *Exp Cell Res* 322:355–364. <https://doi.org/10.1016/j.yexcr.2014.02.009>.
18. Suh HN, Kim MJ, Jung YS, Lien EM, Jun S, Park JI. 2017. Quiescence exit of Tert(+) stem cells by Wnt/beta-catenin is indispensable for intestinal regeneration. *Cell Rep* 21:2571–2584. <https://doi.org/10.1016/j.celrep.2017.10.118>.
19. Cavallo RA, Cox RT, Moline MM, Roose J, Polevoy GA, Clevers H, Peifer M, Bejsovec A. 1998. Drosophila Tcf and Groucho interact to repress Wingless signalling activity. *Nature* 395:604–608. <https://doi.org/10.1038/26982>.
20. Liu X, Lu R, Wu S, Sun J. 2010. Salmonella regulation of intestinal stem cells through the Wnt/beta-catenin pathway. *FEBS Lett* 584:911–916. <https://doi.org/10.1016/j.febslet.2010.01.024>.
21. Wang J, Gong L, Zhang W, Chen W, Pan H, Zeng Y, Liang X, Ma J, Zhang G, Wang H. 2020. Wnt/beta-catenin signaling pathway inhibits porcine reproductive and respiratory syndrome virus replication by enhancing the nuclear factor-kappaB-dependent innate immune response. *Vet Microbiol* 251:108904. <https://doi.org/10.1016/j.vetmic.2020.108904>.
22. Zhou JY, Lin HL, Wang Z, Zhang SW, Huang DG, Gao CQ, Yan HC, Wang XQ. 2020. Zinc L-Aspartate enhances intestinal stem cell activity to protect the integrity of the intestinal mucosa against deoxynivalenol through activation of the Wnt/beta-catenin signaling pathway. *Environ Pollut* 262:114290. <https://doi.org/10.1016/j.envpol.2020.114290>.
23. Li Y, Yang N, Chen J, Huang X, Zhang N, Yang S, Liu G, Liu G. 2020. Next-generation porcine intestinal organoids: an apical-out organoid model for swine enteric virus infection and immune response investigations. *J Virol* 94:e01006-20. <https://doi.org/10.1128/JVI.01006-20>.
24. Crawford SE, Ramani S, Blutt SE, Estes MK. 2021. Organoids to dissect gastrointestinal virus-host interactions: what have we learned? *Viruses* 13:999. <https://doi.org/10.3390/v13060999>.
25. Sato T, van Es JH, Snippert HJ, Stange DE, Vries RG, van den Born M, Barker N, Shroyer NF, van de Wetering M, Clevers H. 2011. Paneth cells constitute the niche for Lgr5 stem cells in intestinal crypts. *Nature* 469:415–418. <https://doi.org/10.1038/nature09637>.
26. Fevr T, Robine S, Louvard D, Huelsken J. 2007. Wnt/beta-catenin is essential for intestinal homeostasis and maintenance of intestinal stem cells. *Mol Cell Biol* 27:7551–7559. <https://doi.org/10.1128/MCB.01034-07>.
27. Sato T, Vries RG, Snippert HJ, van de Wetering M, Barker N, Stange DE, van Es JH, Abo A, Kujala P, Peters PJ, Clevers H. 2009. Single Lgr5 stem cells build crypt-villus structures in vitro without a mesenchymal niche. *Nature* 459:262–265. <https://doi.org/10.1038/nature07935>.
28. Dutta D, Clevers H. 2017. Organoid culture systems to study host-pathogen interactions. *Curr Opin Immunol* 48:15–22. <https://doi.org/10.1016/j.coi.2017.07.012>.
29. Yin L, Liu X, Hu D, Luo Y, Zhang G, Liu P. 2021. Swine enteric coronaviruses (PEDV, TGEV, and PDCoV) induce divergent interferon-stimulated gene responses and antigen presentation in porcine intestinal enteroids. *Front Immunol* 12:826882. <https://doi.org/10.3389/fimmu.2021.826882>.
30. Pelaseyed T, Bergstrom JH, Gustafsson JK, Ermund A, Birchenough GM, Schutte A, van der Post S, Svensson F, Rodriguez-Pineiro AM, Nystrom EE, Wising C, Johansson ME, Hansson GC. 2014. The mucus and mucins of the goblet cells and enterocytes provide the first defense line of the gastrointestinal tract and interact with the immune system. *Immunol Rev* 260:8–20. <https://doi.org/10.1111/imr.12182>.
31. van der Flier LG, Clevers H. 2009. Stem cells, self-renewal, and differentiation in the intestinal epithelium. *Annu Rev Physiol* 71:241–260. <https://doi.org/10.1146/annurev.physiol.010908.163145>.
32. Jiang H, Patel PH, Kohlmaier A, Grenley MO, McEwen DG, Edgar BA. 2009. Cytokine/Jak/Stat signaling mediates regeneration and homeostasis in the Drosophila midgut. *Cell* 137:1343–1355. <https://doi.org/10.1016/j.cell.2009.05.014>.
33. Farin HF, Jordens I, Mosa MH, Basak O, Korving J, Tauriello DV, de Punder K, Angers S, Peters PJ, Maurice MM, Clevers H. 2016. Visualization of a short-range Wnt gradient in the intestinal stem-cell niche. *Nature* 530:340–343. <https://doi.org/10.1038/nature16937>.
34. Clevers H. 2013. The intestinal crypt, a prototype stem cell compartment. *Cell* 154:274–284. <https://doi.org/10.1016/j.cell.2013.07.004>.
35. Clevers H, Nusse R. 2012. Wnt/beta-catenin signaling and disease. *Cell* 149:1192–1205. <https://doi.org/10.1016/j.cell.2012.05.012>.
36. Lindemans CA, Calafiore M, Mertelsmann AM, O'Connor MH, Dudakov JA, Jenq RR, Velardi E, Young LF, Smith OM, Lawrence G, Ivanov JA, Fu YY, Takashima S, Hua G, Martin ML, O'Rourke KP, Lo YH, Mokry M, Romera-Hernandez M, Cupedo T, Dow L, Nieuwenhuis EE, Shroyer NF, Liu C, Kolesnick R, van den Brink MRM, Hanash AM. 2015. Interleukin-22 promotes intestinal-stem-cell-mediated epithelial regeneration. *Nature* 528:560–564. <https://doi.org/10.1038/nature16460>.
37. Zhao X, Ma L, Dai L, Zuo D, Li X, Zhu H, Xu F. 2020. TNF α promotes the malignant transformation of intestinal stem cells through the NF κ B and Wnt/betacatenin signaling pathways. *Oncol Rep* 44:577–588. <https://doi.org/10.3892/or.2020.7631>.
38. Huang X, Chen J, Yao G, Guo Q, Wang J, Liu G. 2019. A TaqMan-probe-based multiplex real-time RT-qPCR for simultaneous detection of porcine enteric coronaviruses. *Appl Microbiol Biotechnol* 103:4943–4952. <https://doi.org/10.1007/s00253-019-09835-7>.